



TNAP expressing adventitial pericytes contribute to myogenesis during foetal development

I. Fancello^a, S. Willett^a, C. Castiglioni^a, S. Amer^a, S. Santoleri^a, L. Bragg^a, F. Galli^a, G. Cossu^{a,b,c,*}

^a Division of Cell Matrix Biology & Regenerative Medicine, FBMH, University of Manchester, UK

^b Institute of Experimental Neurology, Division of Neurosciences, Ospedale San Raffaele, Milan, Italy

^c Experimental and Clinical Research Center, Charité Medical Faculty, Max Delbrück Center Berlin, Germany

ARTICLE INFO

Keywords:

Pericytes

Skeletal myogenesis

Lineage tracing

ABSTRACT

Objective: During growth and differentiation of skeletal muscle, cell types other than canonical myoblasts can be recruited to a myogenic fate. Among these, TNAP+ pericytes can differentiate into skeletal or smooth muscle cells during postnatal growth and contribute to muscle regeneration. However, their role in muscle development has not been investigated. This study aims to characterise pericyte fate choices during embryonic and foetal myogenesis, occurring in the second half of gestation.

Approach and results: Using Cre-loxP lineage tracing with multiple reporters including the multicolor fluorescent Confetti, we labelled TNAP+ precursors *in vivo* and assessed the smooth or skeletal muscle differentiation in their lineage at a perinatal stage. We found that TNAP+ cells contribute *in vivo* to skeletal and smooth muscle cells, as well as other pericytes, also during pre-natal muscle development. The resulting clones showed that such fate choices are likely to depend on distinct unipotent progenitors rather than multipotent progenitors. In addition, we isolated and differentiated *in vitro* foetal cells derived from TNAP+ precursors, which showed that they are not spontaneously myogenic unless co-cultured with other skeletal muscle cells.

Conclusions: This work extends our understanding of the differentiative potency of these non-canonical skeletal muscle progenitors during prenatal life, with a view to a future application of this knowledge to optimise cell therapies for muscle wasting disorders.

1. Introduction

Pericytes are mural cells located at the interface of micro-vasculature with surrounding tissues. They maintain vascular stability and permeability, and regulate development, maturation and regeneration of the vessels [1,2]. Pericytes have been proposed to be the *in vivo* counterpart of mesangioblasts, vessel-associated mesenchymal progenitors forming smooth or skeletal muscle *in vitro* and *in vivo* [3,4,5]. Indeed, several pericyte types have been reported as able to differentiate into other cell types of the surrounding mesoderm tissues. For example, pericytes expressing Tissue Non-Specific Alkaline Phosphatase (TNAP) [6,7], Nestin [8], Neural Glial Factor 2 (NG2) [8,9], or EphA7 [10,11], have shown the ability to form cells of mesenchymal lineages, including

skeletal muscle upon *in vivo* transplantation. Lack of unique markers hampers a definitive characterization of pericytes which would facilitate their isolation, *in vitro* expansion and utilization in cell therapy protocols, given their differentiation potency (especially towards skeletal muscle) and their ability to contribute to angiogenesis to support regenerating tissues. Unlike other pericyte markers [12,13], TNAP is expressed in mouse skeletal muscle by adventitial pericytes and endothelial cells only [3,5,7]. Therefore, previous work that used TNAP as a marker for the lineage tracing of adventitial pericytes revealed that TNAP+ perivascular cells possess skeletal myogenic potency *in vitro* and *in vivo* after birth, contributing to physiological myofiber growth and to regeneration in the context of acute or chronic muscle damage [6,7]. However, the wide expression of TNAP in the embryo outside of skeletal

Abbreviations: TNAP, Tissue Non-specific Alkaline Phosphatase; NG2, Neural Glial factor 2; β -gal, β -galactosidase; skMyHC, skeletal Myosin Heavy Chain; Pax7, paired box protein 7; SM22, smooth muscle protein 22; CD31, cluster of differentiation 31; smMyHC, smooth Myosin Heavy Chain.

* Corresponding author at: Division of Cell Matrix Biology & Regenerative Medicine, Faculty of Biology, Medicine and Health, University of Manchester, Michael Smith Building, D.4316, Oxford Road, M13 9PL Manchester, UK.

E-mail address: giulio.cossu@manchester.ac.uk (G. Cossu).

<https://doi.org/10.1016/j.vph.2025.107489>

Received 26 August 2024; Received in revised form 27 February 2025; Accepted 14 March 2025

Available online 15 March 2025

1537-1891/Crown Copyright © 2025 Published by Elsevier Inc. This is an open access article under the CC BY license (<http://creativecommons.org/licenses/by/4.0/>).

muscle [14,15], and the lack of a strategy for limited clonal tracing have so far hampered the investigation of the myogenic potency of TNAP+ cells before birth. Here, to explore their role during pre-natal skeletal muscle development, we performed lineage tracing in *TNAP-Cre^{ERT2}* mice at the foetal stage with the use of low doses of Tamoxifen and clonal tracing approaches, including the multi-fluorescent *Brainbow 2.1* “Confetti” reporter [16,17,18]. This strategy allowed us to follow low-frequency clones of a small number of TNAP+ progenitors and to study their fate choices in the developing muscle. Our data show that TNAP+ progenitors contribute to the formation of myofibers, vascular smooth muscle cells and other pericytes, but show no evidence that progenitors are clonally tri-potent or bi-potent during development. In addition, we found that foetal TNAP+ progenitors require the proximity of skeletal muscle cells to achieve myogenic differentiation, unlike their post-natal counterparts.

2. Materials and methods

2.1. Mouse models and tamoxifen treatment

Lineage tracing was performed according to the UK Animals (Scientific Procedures) Act (1986), under Home Office Licenses PPL PDB0CF0C2 and PPL PP8863485. The employed strains were *TNAP-Cre^{ERT2}* [ref. 7], *NG2-Cre^{ERT2}* (Jackson Laboratories), *R26R-NZG* [ref. 7], *R26R-tdTomato* (Jackson Laboratories) and *R26R-Confetti* (Jackson Laboratories). For prenatal labelling, pregnant females received at E11.5 or E14.5 one intraperitoneal injection of 1.0 mg of tamoxifen (Sigma T5648) with 0.5 mg of progesterone (Sigma P7556) diluted in corn oil. Foetuses were then harvested at E17.5. Wild-type foetuses from CD1 mice were collected for histology at E11.5 and E14.5. As negative controls, wild-type mice were crossed to reporter mice: 1 foetus for each reporter strain was analysed at E11.5 and E14.5. No reporter gene expression was observed as expected. For *TNAP-Cre^{ERT2}; R26R-NZG* lineage tracing, $N = 3$ foetuses were used for analysis. The preliminary quantitative counts were generally performed on a maximum of 10 randomly selected sections for each foetus. If deemed necessary 10 additional sections were examined. For *TNAP-Cre^{ERT2}; R26R-Confetti* lineage tracing, $N = 3$ foetuses were used for further analysis, and the preliminary quantitative counts were performed as described above. The very low fertility of the crosses limited the number of foetuses available. For *TNAP-Cre^{ERT2}; R26R-tdTomato* foetal lineage tracing, whole litters of 6–7 foetuses were collected and employed for tissue digestion and cell dissociation for subsequent culture ($N = 2$ experiments). For histological analysis, $N = 3$ foetuses were used as described above. For postnatal labelling, mouse pups received subcutaneous injections of 32.5 mg/kg of tamoxifen diluted in corn oil, repeated for 3 consecutive days at P6, P7 and P8 after birth. The mice were then culled at P15 to isolate hindlimb and forelimb skeletal muscles. The muscles from 3 mouse pups from the same litter were employed for tissue digestion and cell dissociation for subsequent culture ($N = 2$ experiments).

2.2. X-gal staining

TNAP-Cre^{ERT2}; R26R-NZG foetuses were fixed with paraformaldehyde (PFA) 4% at RT for 5 h. The samples were incubated in X-Gal solution (Roche 10745740001) O/N at 37°C, washed in PBS, dehydrated with increasing sucrose concentrations (7–15–30%) and finally frozen within OCT with isopentane/liquid nitrogen. Prior to freezing, images were acquired with the ZEISS Axio Zoom V16 stereomicroscope.

2.3. Immunofluorescence

Harvested embryos were fixed with PFA 4% at RT for 3 (E11.5), 4 (E14.5), or 5 h (E17.5) and then frozen within OCT in isopentane/liquid nitrogen. For Pax7 staining, cryosections were permeabilized with

methanol at -20°C for 10 min, then incubated in citrate buffer (10 mM citrate, 0.05% Tween, pH 6.0) in boiling water for 15 min. For all other staining, cryosections were fixed with PFA 4% for 10 min at RT, then permeabilized with PBS-Triton X-100 0.25% for 30 min at RT and saturated with 10% goat serum for 1 h at RT. For mouse-on-mouse antigen detection, the samples were additionally incubated with F_{ab} goat anti-mouse antibody fragments (Jackson ImmunoResearch 115–007–003) diluted 1:100 in PBS, for 1 h at RT. Primary antibodies were incubated O/N at 4°C in saturation buffer, using the following: anti-skMyHC, (1:2, MF20 DSHB), anti-Pax7 (1:3, DSHB), anti-MyoD (1:40, Dako M3512), anti-TNAP (1:40, Thermo Fisher PA5–47419), anti-NG2 (1:50, R&D MAB6689), anti-laminin (1:200, Sigma L9393), anti- β -gal (1:100, MP Biomedicals 0855976), anti-smMyHC (1:100, Abcam Ab125884), anti-SM22 (1:200, Abcam Ab14106), anti-CD31 (1:100, Abcam Ab28364). Sections were then washed and incubated for 1 h at RT with secondary antibodies diluted 1:500, with the addition of Hoechst 33258 (Thermo Fisher) 1:1000. Samples were then washed and mounted, and imaging was performed with ZEISS Axio Imager M2 fluorescence microscope and Leica TCS SP8 Upright and ZEISS LSM 880 Airy Upright confocal microscopes. Unless otherwise specified, $N = 3$ foetuses were studied for experimental points and a maximum of 10 non serial sections from one of these foetuses (we did not observe inter-foetal variability) were used to identify and characterise clones.

2.4. Cell isolation from foetuses

After foetuses were isolated in PBS + 1% penicillin/streptomycin (Pen-Strep) and finely minced, the resulting pulp was incubated with 1% Collagenase D (Roche 11088866001), 10 $\mu\text{l}/\text{ml}$ DNaseI (Roche 11284932001) in Hank Balanced Salt Solution with $\text{Ca}^{2+}/\text{Mg}^{2+}$ (HBSS, Gibco 14025–050) for 10 min at 37°C in shaking bath, for 3 repeated cycles of digestion. The supernatant was collected and filtered with 100, 70 and 40 μm cell strainers, and the enzymatic activity blocked with recovery buffer composed of 10% BSA (Sigma A2153), 1% Pen-Strep, 1 mM EDTA (Sigma E7889) in HBSS without $\text{Ca}^{2+}/\text{Mg}^{2+}$ (Sigma 14175–053). Samples were then centrifuged at 500g for 30 min and the pellet was resuspended as later described.

2.5. Cell isolation from adult skeletal muscles

Individual hindlimb and forelimb skeletal muscles were dislocated by pinching the tendons and longitudinally cutting the muscle fascia. Muscles were cleaned and washed in PBS + 1% Pen-Strep, then minced to fine pieces of 3 mm^3 of size. The resulting pulp was dissociated with 1% Collagenase D, 2.4 U/ml Dispase II (Gibco 17105–041), 10 $\mu\text{l}/\text{ml}$ DNaseI, 2 $\mu\text{l}/\text{ml}$ EDTA in HBSS with $\text{Ca}^{2+}/\text{Mg}^{2+}$ for 45 min at 37°C in shaking bath, for one cycle of digestion. The supernatant was processed as above. Samples were then centrifuged at 310g for 6 min at 4°C and the pellet was resuspended as later described.

2.6. Cell sorting

The cells were resuspended in sorting buffer containing 20 mM HEPES pH 7.0, 1 mM EDTA, 1% BSA, 1% Pen-Strep, 1:100 DNaseI in HBSS without $\text{Ca}^{2+}/\text{Mg}^{2+}$ and filtrated again with 40 μm strainer. FACS sorting was carried out at 4°C on Bigfoot Cell Sorter (Invitrogen) or Influx Cell Sorter (BD). Sorted cells were collected in PBS with 50% FBS, then centrifuged at 1800 rpm for 10 min and used as follows.

2.7. Feeder layer preparation and differentiation assay

Immortalized C2C12 mouse myoblasts were cultured with D10, that is DMEM-high glucose (Sigma, D5796) with 10% FBS, 1% Pen-Strep, 1% sodium pyruvate and kept at 37°C with 20% O_2 . For myoblast differentiation, C2C12 cells were plated in 48-well plates coated with Collagen I (Sigma, C8919), and allowed to reach 70% confluence before

changing the medium to DMEM-high glucose with 2% Horse Serum (HS), 1% Pen-Strep and 1% sodium pyruvate. Medium was substituted fresh every 48 h and kept for 5–6 days before using C2C12 as feeder layers. After sorting of primary mouse cells, part of them were resuspended in D4, that is DMEM-high glucose with 4% HS, 1% Pen-Strep and 1% sodium pyruvate and seeded at low density (100 cells/well) in the plates containing differentiated C2C12. Another part was resuspended in D10 and seeded alone in collagen-coated 48-well plates at high density (up to 20,000 cells/well). After 24 h, medium was changed to D4, substituted fresh every 48 h. All experimental cultures were kept at 37°C with 5 % O₂ and fixed after 6 days.

2.8. Immunocytochemistry (ICC)

Cultures were washed with PBS, then fixed with PFA 4% for 10 min at RT. Immunocytochemistry was carried out as described in Dellavalle et al. (2007) [ref. 6]. The primary antibodies used in this work were: anti-skMyHC (1:2, MF20 DSHB), anti-smMyHC (1:100, Abcam Ab125884).

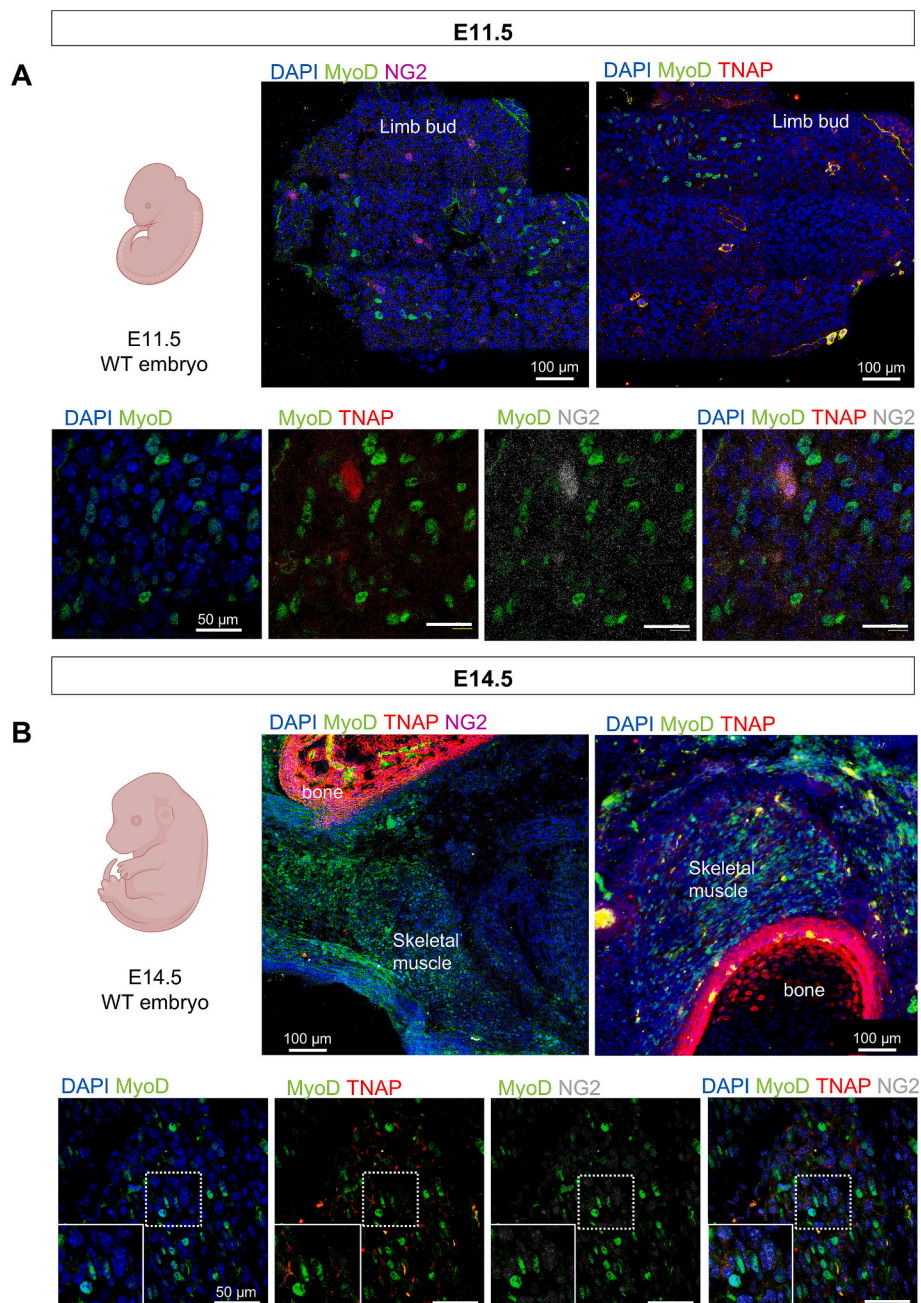


Fig. 1. Expression of TNAP or NG2 in developing muscle. (A) Analysis performed on wt embryo at E11.5. IF on 10 μ m cryosections, at the level of forelimbs, showing no co-localisation of MyoD signal (green) with either NG2 (magenta or grey) or TNAP (red), with nuclei counterstained with DAPI (blue). Same staining at higher magnification at the bottom. (B) Analysis performed on wt foetus at E14.5. IF on 10 μ m cryosections, at the level of forelimbs, showing no co-localisation of MyoD signal (green) with either NG2 (magenta or grey) or TNAP (red), with nuclei counterstained with DAPI (blue). Same staining at higher magnification at the bottom, with highlight in the framed area in the bottom left corner. (For interpretation of the references to colour in this figure legend, the reader is referred to the web version of this article.)

3. Results

3.1. Embryonic and foetal myoblasts do not express TNAP or NG2

To ensure reliability of lineage tracing and to avoid inadvertently labelling of canonical myogenic cells, we investigated the possible co-expression of TNAP with the myogenic marker MyoD at E11.5 and E14.5. We also examined co-expression of the mural cell marker NG2 (Neural Glial Factor 2) with MyoD both in limbs and trunk. At E11.5, transversal sections of the developing forelimb bud of wild-type embryos (from CD1 pregnant females) revealed expression of MyoD in clusters of cells that were not labelled by TNAP or NG2 antibodies (Fig. 1A). Similar sections obtained from embryos at the later stage of E14.5 showed that the clusters of MyoD+ cells were organised in areas corresponding to the developing limb flexor and extensor muscles near TNAP+ structures such as the bone, which was indeed strongly stained (Fig. 1B). At this stage, we did not detect NG2 expression in developing skeletal muscles. Instead, TNAP was present in cells scattered throughout the muscle, but the TNAP+ cytoplasmic staining did not co-localise with MyoD+ nuclei.

3.2. Embryonic TNAP+ progenitors give rise to myogenic progeny in vivo also in developing skeletal muscle

TNAP-Cre^{ERT2} mice were crossed with either R26R-NZG or R26R-Confetti reporter mice to generate TNAP-Cre^{ERT2}; R26R-NZG and TNAP-Cre^{ERT2}; R26R-Confetti fetuses. We achieved timely expression of the reporters by administration of tamoxifen to pregnant mice at time points corresponding to primary (E11.5) or secondary myofiber formation (E14.5), thus allowing to follow the fate of TNAP+ cells in developing skeletal muscles before birth (collection at E17.5). Labelled cells expressing either nuclear β -galactosidase reporter (nLacZ), or a random combination of CFP, GFP, YFP or RFP, were detected in the collected foetal samples by fluorescence microscopy, to assess position and frequency, marker expression and differentiation into smooth or skeletal muscle *in vivo*. Following the scheme in Fig. 2A, TNAP-Cre^{ERT2}; R26R-NZG pregnant dams received one intra-peritoneal injection of tamoxifen at E11.5, and were culled at E17.5 to analyse the fetuses for the expression of β -gal. X-Gal staining allowed to first find cells derived from TNAP+ precursors in the skin layer from an early stage of collection already (E14.5) (Fig. 2B). At E17.5, the labelled cells appeared widely distributed in organs such as kidney and liver, as well as in the cardiac muscle and in mesenchymal tissues such as cartilage, bone and dermis, with fewer clones detected in vessels and skeletal muscle (Fig. 2C). Cryosections of the X-gal+ fetuses revealed abundant localisation of labelled nuclei in the upper trunk and forelimbs of the fetus (Fig. 2D), with an ordered and aligned distribution within the muscle tissue (Fig. 2E). Subsequent immunofluorescence analysis allowed to localise many of the aligned labelled nuclei inside myofibers expressing skeletal myosin heavy chain (skMyHC, Fig. 2G). Preliminary quantification of signal co-localisation indicated that in this model almost 40% of β -gal+ nuclei are located within skMyHC+ differentiated myofibers (Fig. 2F).

3.3. Clonal tracing shows that embryonic TNAP+ progenitors contribute to developing myofibers and, sporadically, to Pax7+ myoblasts

To identify possible bi or tri-potent progenitors at the clonal level, we administered tamoxifen to TNAP-Cre^{ERT2}; R26R-Confetti mice using the same protocol as previously described (labelling at E11.5 and analysis at E17.5) (Fig. 3A). Since the efficiency of recombination is not very high [7], we expect a small number of single TNAP+ cells to also express one out of four possible fluorescent proteins, originated by Cre random recombination in the Confetti reporter transgene inherited by the progeny (Fig. 3B). We then screened the resulting fetuses for reporter activation, focusing on the detection of nuclear GFP and cytoplasmic RFP (Fig. 3C). Screening of organs that are known to robustly express

TNAP, such as kidney and testis, showed labelling as expected (Fig. 3C). In Fig. 3D, Confetti signals such as YFP were found in differentiated myofibers expressing skMyHC, confirming the result of the tracing from TNAP-Cre^{ERT2}; R26R-NZG and the myogenic potency of these embryonic precursor cells. Myogenic differentiation into multinucleated skMyHC+ cells was detected even when tamoxifen was administered later (E14.5), resulting in labelling of foetal but not embryonic TNAP+ precursors (Supplementary Fig. S1). At all times analysed, we did not detect clones marked by a single fluorochrome that comprise both muscle fibres and smooth muscle or other mesoderm cells, suggesting that at the time of labelling the majority of TNAP+ cells had already adopted a specific fate. It is possible that a minority of cells derived from a bi or tri-potent progenitor may have been missed in the analysis because of their low frequency. Subsequently, we wondered whether the lineage of embryonic TNAP+ cells may contribute to myogenesis by converting into Pax7+ myoblasts or satellite cells, canonically involved in the generation of new myofibers during foetal and postnatal muscle growth. Cryosections of TNAP-Cre^{ERT2}; R26R-Confetti fetuses were used for immunofluorescence staining of Pax7 in foetal skeletal muscle. Fig. 3E shows the distribution of Pax7 nuclear expression in a region of the E17.5 fetus corresponding to skeletal muscle. It is possible to observe sporadic co-localisation of nuclear GFP signal with Pax7, adjacent to muscle fibre but outside the basal laminin. Location of double positive cells outside of newly formed basal lamina, suggests that these are late differentiating foetal myoblasts and not mature satellite cells. Preliminary quantification of Pax7+/GFP+ cells indicates that a very limited percentage (<4%) of the cells traced in TNAP-Cre^{ERT2}; R26R-Confetti express Pax7 at E17.5 (Fig. 3F).

3.4. Embryonic TNAP+ progenitors contribute to skeletal muscle cells, smooth muscle cells and pericytes but from different progenitor cells

The majority of traced cells coming from TNAP+ precursors did not contribute to skeletal muscle. In order to understand whether they acquire smooth muscle or pericyte alternative fates as they do after birth, we used E17.5 TNAP-Cre^{ERT2}; R26R-Confetti fetuses that received tamoxifen at E11.5 (Fig. 4A) to immunostaining for transgelin (SM22, smooth muscle marker), Neural Glial Factor 2 (NG2, pericyte marker), and CD31 (PECAM, endothelial cell marker). The results showed GFP+ clones in areas corresponding to skeletal muscle, where they were found close to the vessels and co-localising with SM22+ smooth muscle cells (Fig. 4B) or NG2+ mural cells (Fig. 4C). Indeed, an average of 7% of the counted cells expressed SM22, indicating smooth muscle differentiation, while an average of 20% of them expressed NG2 (Fig. 4D). However, while clones corresponding to skeletal muscle cells, smooth muscle cells and other pericytes were found, no mixed clones were observed, suggesting that TNAP+ cells have already chosen a smooth or a skeletal differentiation pathway at the time of Cre activation (E11.5).

3.5. Foetal NG2+ cells may also undergo myogenic differentiation in developing skeletal muscle

NG2 is a typical marker of pericytes whose expression is widely used to identify this cell type *in vivo* [1,12]. During development, other cells including neural cells, chondroblasts and osteoblasts [19,20,21] also express NG2, but not MyoD+ skeletal myoblasts (Fig. 1). To compare the possible fate choices of NG2+ cells with TNAP+ cells *in vivo* during skeletal muscle formation, we additionally traced the lineage of foetal NG2+ pericytes in NG2-Cre^{ERT2}; R26R-tdTomato mice. Precursors labelled at E14.5 led to derivatives that, similarly to their TNAP+ lineage counterpart, colonised at E17.5 both pericyte and, to a much lower extent, myofiber compartments, suggesting a low myogenic contribution of the NG2+ lineage at this stage (Supplementary Fig. S2).

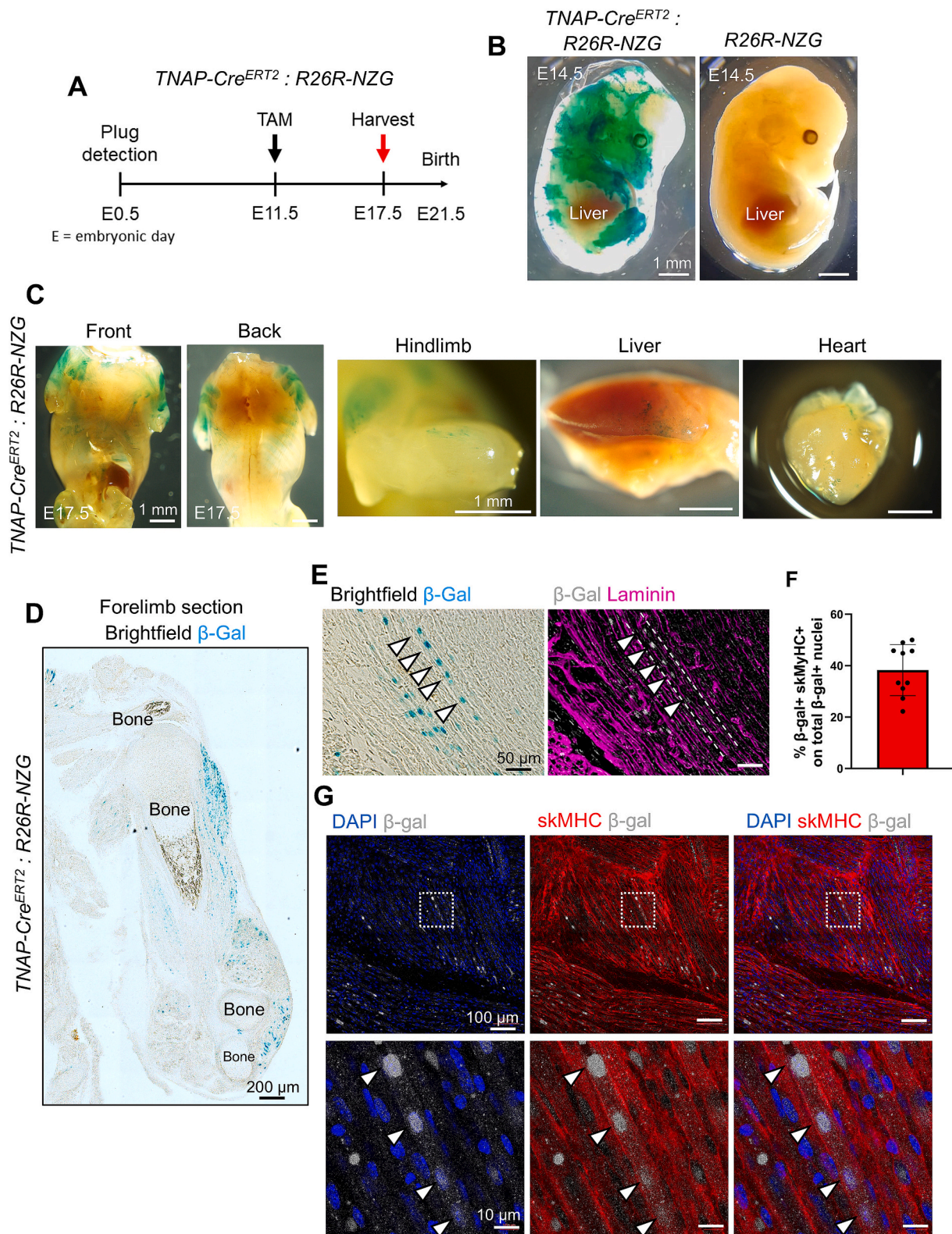


Fig. 2. Lineage tracing in *TNAP-Cre^{ERT2} ; R26R-NZG* mice.

(A) Experimental protocol of the study with *TNAP-Cre^{ERT2} ; R26R-NZG* mice. (B) X-gal+ and X-gal- (control) embryos collected at E14.5 for preliminary screening. (C) Front and back pictures of E17.5 X-gal+ foetus without skin, with close-ups of hindlimb muscles, liver and heart. (D) Brightfield cryosection of E17.5 X-gal+ foetus, detail of the forelimb with β -gal in blue. (E) IF on 10 μ m cryosections of *TNAP-Cre^{ERT2} ; R26R-NZG* foetus at E17.5, highlighting the alignment of β -gal+ nuclei (blue or white) inside myofiber basal lamina stained with laminin (magenta). (F) Quantification (%) of β -gal+ nuclei in skMyHC+ myofibers on total number of β -gal+ nuclei per field of view. Labelled nuclei were counted from 10 fields of view, $N = 3$ foetuses, with ImageJ Fiji; data were used for graph creation with GraphPad Prism 10, and reported as individual points with mean \pm SD. Data points from one representative embryo are shown. (G) IF on 10 μ m cryosections of *TNAP-Cre^{ERT2} ; R26R-NZG* foetus at E17.5, staining β -gal (white) and skMyHC (red) with DAPI counterstained nuclei (blue). In (E) and (G), white arrows indicate aligned β -gal+ nuclei. (For interpretation of the references to colour in this figure legend, the reader is referred to the web version of this article.)

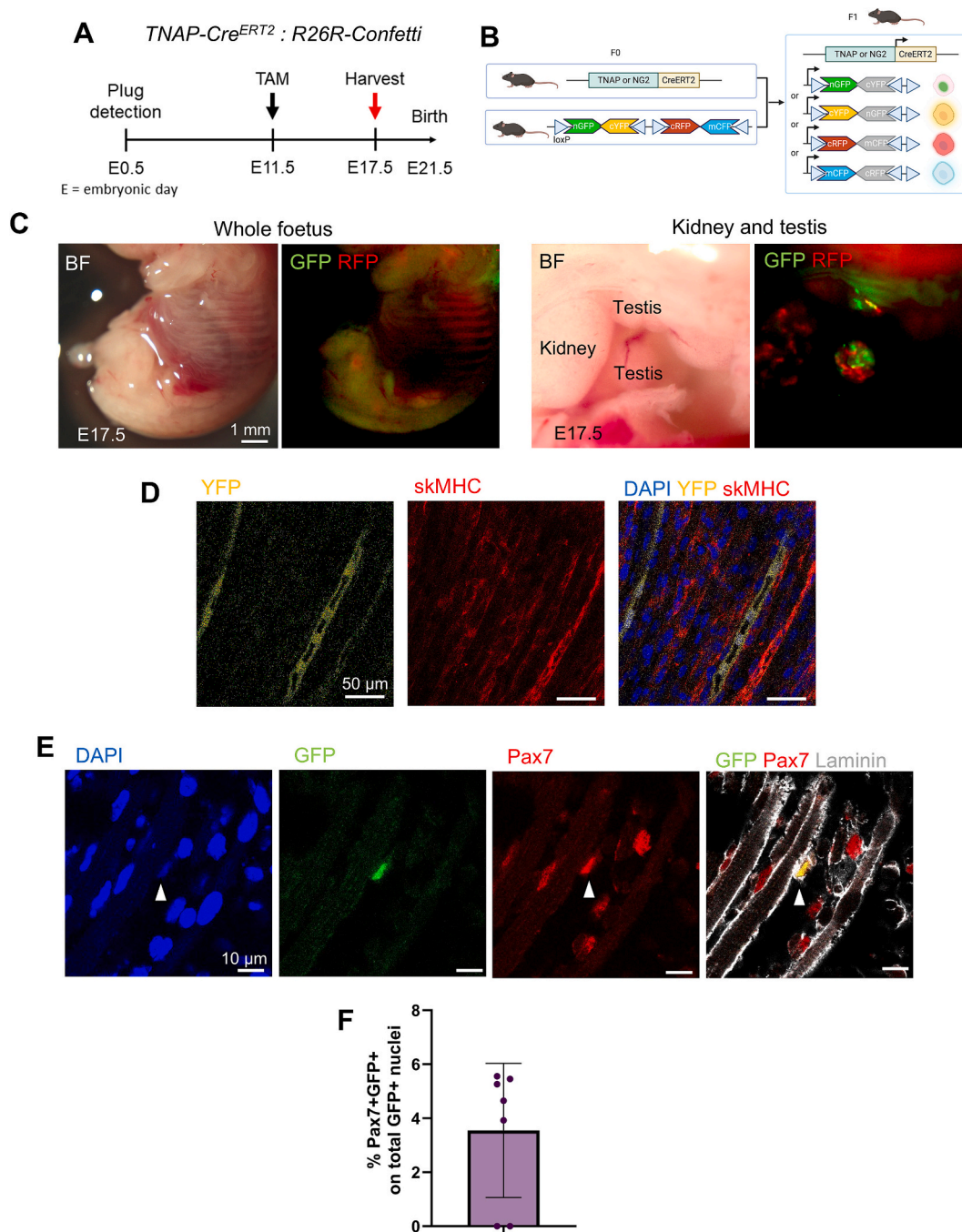


Fig. 3. Lineage tracing of TNAP+ cells in *TNAP-Cre^{ERT2}; R26R-Confetti* mice.

(A) Experimental protocol of the study with *TNAP-Cre^{ERT2}* mice. (B) Scheme representing Cre and reporter mouse crossings, with outcomes of Confetti recombination. (C) Brightfield (BF) and fluorescence (GFP/RFP) pictures of E17.5 Confetti foetus without skin, showing lateral view and close-ups of kidney and testis. (D) IF on 10 μm cryosections of *TNAP-Cre^{ERT2}; R26R-Confetti* foetus at E17.5, showing YFP+ (yellow) myofibers stained for skMyHC (red), with DAPI counterstained nuclei (blue). (E) IF on 10 μm cryosections of *TNAP-Cre^{ERT2}; R26R-Confetti* foetus at E17.5, showing Pax7+ nuclei (red) in skeletal muscles co-localising with GFP+ nucleus (green), with basal lamina underlined by laminin (grey) and nuclei counterstained with DAPI (blue). (F) Quantification (%) of GFP+ Pax7+ nuclei on total GFP+ nuclei per field of view. Labelled nuclei were counted from 7 fields of view, N = 3 foetuses, with ImageJ Fiji; data were used for graph creation with GraphPad Prism 10, and reported as individual points with mean ± SD. Data points from one representative embryo are shown. (For interpretation of the references to colour in this figure legend, the reader is referred to the web version of this article.)

3.6. Foetal TNAP+ progenitors cultured *in vitro* are not spontaneously myogenic, unlike their post-natal counterpart

To investigate whether the myogenic derivatives of the TNAP+ lineage found *in vivo* are spontaneously myogenic, we examined the *in vitro* cell potency at different stages, in presence or absence of other skeletal muscle cells. Using the experimental schemes shown in Fig. 5A

and B, we induced Cre activation in *TNAP-Cre^{ERT2}; R26R-tdTomato* foetuses or growing pups, obtained by crossing *TNAP-Cre^{ERT2}* driver mice with *R26R-tdTomato* reporter mice. For the developmental stage of analysis, pregnant dams were treated with tamoxifen at E14.5, during foetal myogenesis, and foetuses were harvested at E17.5. For the post-natal stage, *TNAP-Cre^{ERT2}; R26R-tdTomato* pups received tamoxifen at P6–7–8 days of age to induce Cre recombination during muscle growth,

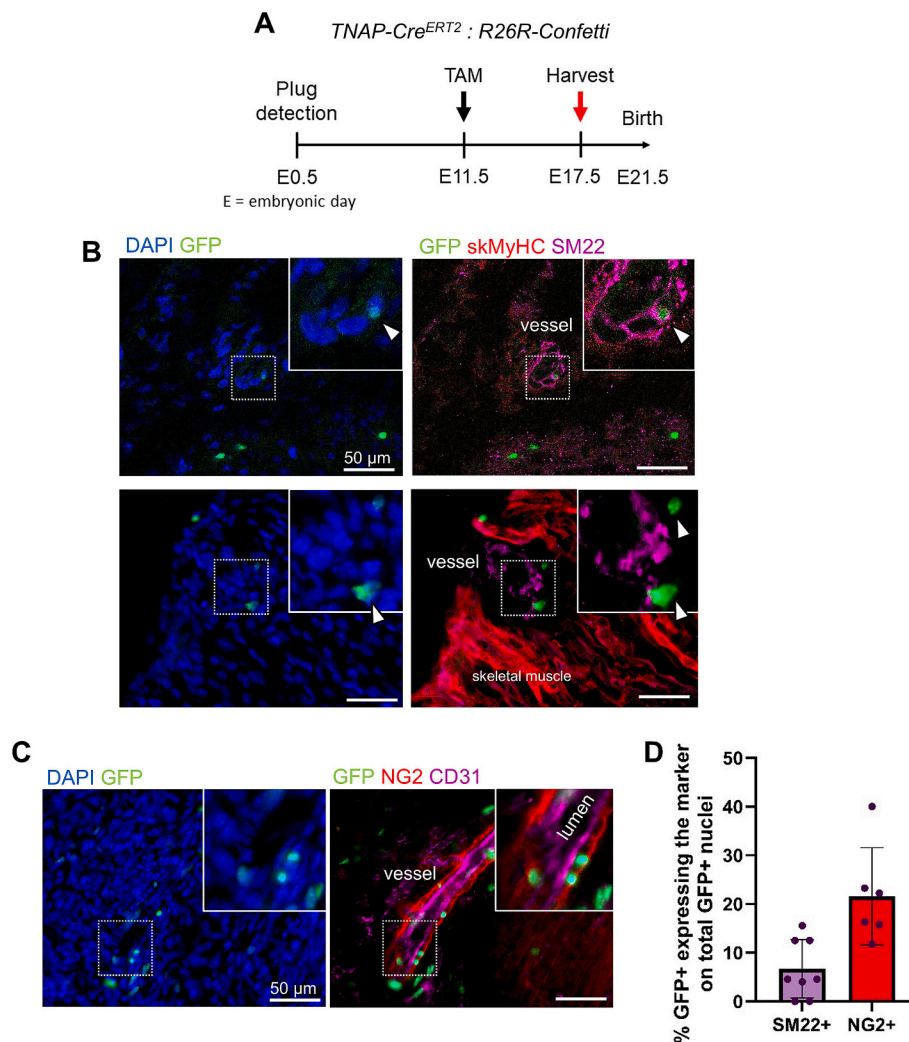


Fig. 4. Smooth muscle and pericyte differentiation of TNAP+ cells.

(A) Experimental protocol of the study with *TNAP-Cre^{ERT2} : R26R-Confetti* mice. (B) IF on 10 μ m cryosections of *TNAP-Cre^{ERT2} : R26R-Confetti* foetus at E17.5, showing groups of GFP+ nuclei (green) indicated by white arrows corresponding or in association with smooth muscle cells expressing SM22 (magenta) but not with skMyHC+ myofibers (red), with DAPI counterstained nuclei (blue). (C) IF on the same sections showing a group of GFP+ nuclei (green) in close association with a CD31+ vessel (magenta), part of which are in the perithelial layer of NG2+ cells (red), with DAPI counterstained nuclei (blue). (D) Quantification (%) of GFP+ SM22+ or GFP+ NG2+ nuclei on the total number of GFP+ nuclei per field of view. Labelled cells were counted from 6 to 8 fields of view, N = 3 foetuses, with ImageJ Fiji; data were used for graph creation with GraphPad Prism 10 and reported as individual points with mean \pm SD. Data points from one representative embryo are shown. (For interpretation of the references to colour in this figure legend, the reader is referred to the web version of this article.)

and hindlimb and forelimb muscles were harvested at P15. Foetal or postnatal samples were then dissociated to obtain a single-cell suspension, then sorted to obtain an enriched population of tdTomato+ cells derived from TNAP+ precursors. Both sorted subsets (foetal and neonatal) were seeded onto plates containing either a feeder layer of differentiated murine skeletal muscle cells (C2C12) or no feeder layer and allowed to differentiate for 6 days. Then, all cultures were fixed and stained by ICC to reveal the degree of skeletal or smooth muscle differentiation by expression of the markers skMyHC and smMyHC (skeletal and smooth myosin heavy chain), respectively. After co-culture with C2C12, foetal cells gave rise to tdTomato+ skMyHC+ myotubes (Fig. 5C), which from a preliminary quantification resulted in an average of 24% of the total tdTomato+ cells (Fig. 5D). On the contrary, in the absence of C2C12, foetal cells did not spontaneously form skMyHC+ myotubes and mostly adopted a smooth muscle fate, as evidenced by smMyHC expression (Fig. 5E). Instead, the assay performed on the post-natal subset indicated that myogenic differentiation of TNAP-derived progenitors after birth does not depend on nearby skeletal muscle cells, as tdTomato+ myotubes were detected in both co-culture

and single culture (Fig. 5F-G).

4. Discussion

In the last twenty years, several cell types, different from dermomyotome-derived myoblasts (*i.e.* Pax- and MRF-) have been identified. These cells are capable of undergoing skeletal myogenesis and contributing to myonuclei in a permissive environment [6,7,8,11,22,23,24]. Among them, TNAP+ pericytes showed myogenic and smooth muscle differentiation during postnatal muscle growth and regeneration [7], indicating them as non-canonical myogenic cells. However, the study of TNAP+ cells lineage during prenatal muscle development remained unexplored. It also remained unclear whether these cells, associated with the vascular niche, may be multipotent towards different mesoderm fates. Independently from TNAP expression, previous work showed that clones from the embryonic aorta also colonise the myotome at a very early stage [25] while explants of embryonic aorta from MLC/1/3F-nLacZ mice opt for a skeletal myogenic fate in the presence of skeletal myoblasts, this effect being potentiated by Noggin

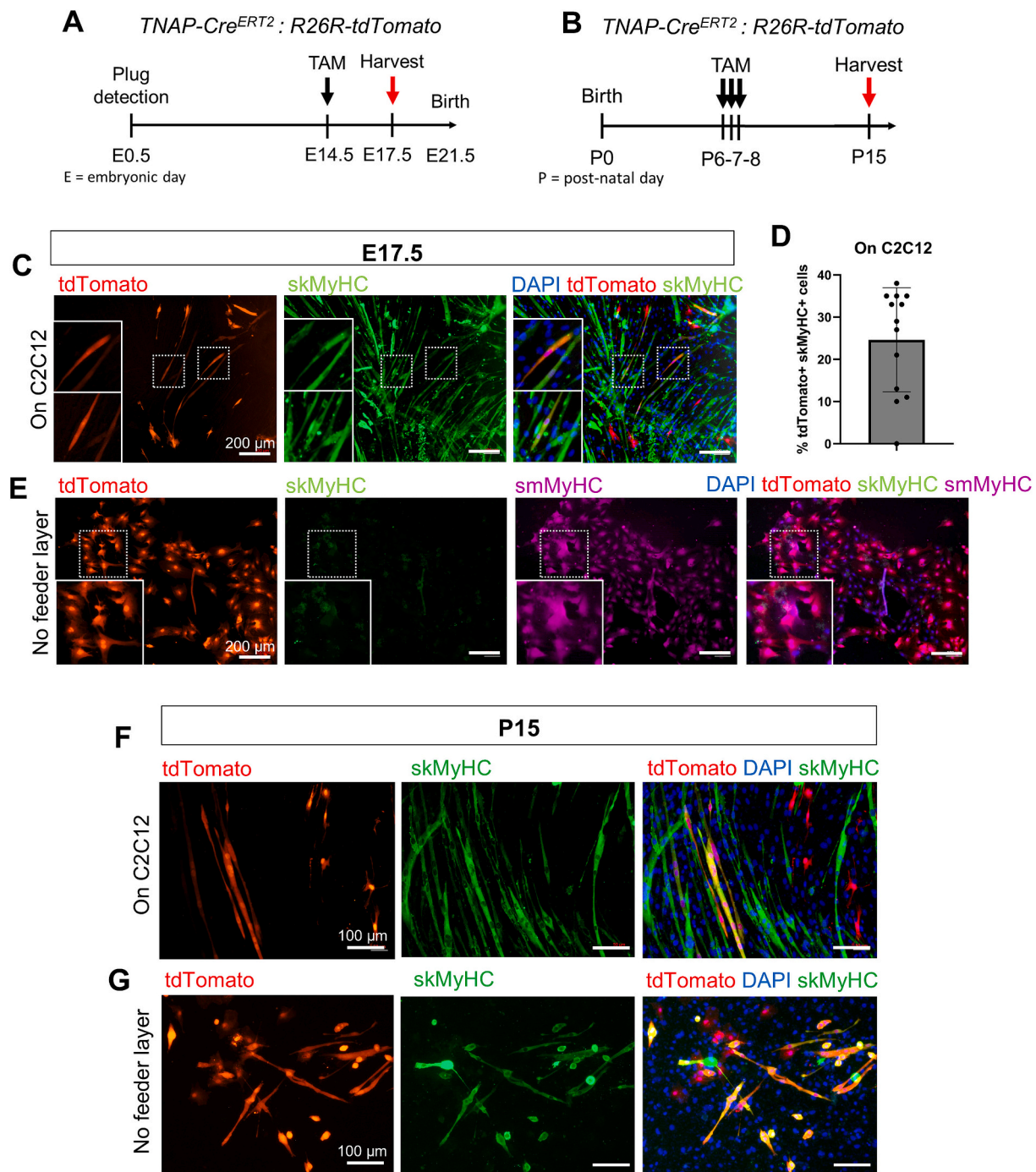


Fig. 5. Effect of skeletal muscle feeder layer on foetal or postnatal TNAP⁺ precursors.

(A) Experimental protocol of the study during foetal development with *TNAP-Cre^{ERT2}; R26R-tdTomato* mice. (B) Experimental protocol of the study during postnatal growth with *TNAP-Cre^{ERT2}; R26R-tdTomato* mice. (C) ICC on sorted foetal tdTomato⁺ (red) cells co-cultured on C2C12, showing DAPI (blue) and skMyHC (green). (D) Quantification (%) of foetal tdTomato⁺ skMyHC⁺ cells on the total tdTomato⁺ cells per field of view in co-cultures of sorted cells and C2C12. 12 fields of view were counted with ImageJ Fiji from $N = 2$ experiments; data were used to create the graph with GraphPad Prism 10, and reported as mean \pm SD. Data points from one representative experiment are shown. (E) ICC on sorted foetal tdTomato⁺ (red) cells cultured alone, showing DAPI (blue), skMyHC (green) and smMyHC (magenta). (F) ICC on sorted postnatal tdTomato⁺ (red) cells co-cultured on C2C12, showing DAPI (blue) and skMyHC (green). (G) ICC on sorted postnatal tdTomato⁺ (red) cells cultured alone, showing DAPI (blue) and skMyHC (green). (For interpretation of the references to colour in this figure legend, the reader is referred to the web version of this article.)

and inhibited by BMP2 [26]. At the molecular level, a competition between Pax3 and FoxN1 dictates the choice between skeletal and smooth muscle [27]. In this work, we used *TNAP-Cre^{ERT2}* mice to follow the lineage of TNAP⁺ cells in developing mouse skeletal muscle, and to analyse their fate choices using a clonal approach with the *Brainbow2.1* “Confetti” reporter. Apart from pericytes, TNAP is expressed in other cell types in the mouse embryo, including endothelial cells and other

mesoderm progenitors [14,15], but expression in skeletal muscle had not been investigated. After showing that expression of TNAP and NG2 does not co-localise with MyoD in wild-type embryos and foetuses, we proceeded to trace the lineage of these progenitors over the course of development. Activation of the multi-fluorescent Confetti reporter was achieved with low doses of Tamoxifen [16,18], aiming at tracking clones (given the low recombination frequency) originating from a small

number of TNAP+ progenitors. Derivatives of embryonic TNAP+ precursors were found to predominantly colonise foetal mesenchymal tissues including cartilage, bone and dermis, consistently with the reported expression of TNAP in these tissues [15]. We found cells derived from TNAP+ progenitors also in foetal myofibers, smooth muscle cells and NG2+ pericytes. Therefore, the results indicate that TNAP+ cells of the skeletal muscle can acquire a myogenic fate and enter the myofiber compartment already from an embryonic and foetal developmental stage. TNAP+ cells contribute to skeletal muscle fibres with approximately 40% of the nuclei from the embryonic TNAP+ lineage found within myofibers, though this is still a small percentage of total muscle nuclei. Myogenic differentiation was confirmed with Confetti clonal labelling, which highlighted the myogenic derivatives with cytoplasmic YFP and RFP staining in myofibers and sporadic nuclear GFP staining in Pax7+ nuclei. Pax7 is a transcription factor typically expressed during development by foetal myoblasts and, later, by satellite cells [28,29]. There are no known markers to distinguish foetal myoblasts from satellite cells, but the location of double labelled cells outside the fibre basal lamina hints that these cells are not mature satellite cells. Thus, the obtained results suggest that embryonic TNAP+ progenitors contribute to foetal myoblasts, although to a very limited extent. Skeletal myogenic potency is observed both in embryonic and foetal TNAP+ cells, as both contribute to myofiber formation. Among the analysed Confetti+ progeny of the studied lineage, it was possible to find derivatives that also underwent a smooth muscle or pericyte fate, thus remaining associated with the vessels. The pericyte fate seems preferred among the two, with 7% expressing the SM22+ smooth muscle marker and 20% expressing only NG2+ pericyte marker. The presence of smooth muscle and pericyte derivatives of TNAP+ precursors was expected in light of the anatomical localisation and the known differentiation potency of vascular progenitors [30]. Cartilage, dermis, bone are other possible cell fates adopted by TNAP+ progenitors that we did not analyse. In all cases, we were unable to identify single clones whose components adopted all the three fate choices (skeletal muscle/smooth muscle/pericyte) or even skeletal/smooth or skeletal/pericyte bipotent progenitors. Therefore, our data suggest that fate choices occur early during development. The Waddington lineage landscape [31] postulates a progressive restriction of fates with subsequent stages of development. However, there is not a general rule on when the fate of a specific progenitor becomes restricted to few, or only one, cell types. For example, in adult skin a multipotent stem cell in the bulge of the hair follicle (generating epidermis, hair and sebaceous glands) coexists with interfollicular unipotent stem cells that only generate keratinocytes [32]. Also, lineage tracing revealed examples of unipotent progenitors such as those of the acinar cells of the pancreas [33].

To compare the differentiative potency of the TNAP+ population with another pericyte population, we additionally traced the lineage of NG2+ pericytes, which are known to modulate myogenesis in satellite cells and directly possess limited myogenic potency in postnatal skeletal muscle [8,9, 34]. Recently it was reported that CD146+/NG2+ myogenic progenitors participate to muscle regeneration [35]. In agreement with this report, and similarly to TNAP+ pericytes, we found that during foetal muscle formation NG2+ cells give rise to other NG2+ pericytes but also undergo limited myogenic differentiation. The phenotypic characterization of the three populations is challenging, except for skeletal myoblasts that express unique markers such as MyoD and Myf5. Pericytes express many markers in common with smooth muscle (SM22, calponin, α -SMA, desmin, etc.) and others in common with skeletal myoblasts (PDGFR β , NG2, and again SM22, α -SMA, desmin, etc.). Recently, a detailed study by Betsholtz group identified several genes that distinguish pericytes from fibroblasts of different types of muscles [36], but unfortunately mature myocytes and smooth muscle were not included in the study, leaving a definitive answer to further investigations.

Myogenic differentiation is initiated in the embryo in response to signals originating from adjacent structures such as neural tube,

notochord and ectoderm [37,38,39,40,41,42], and continues in an environment including Extra-Cellular Matrix (ECM) [43,44,45], growing blood vessels [40,46,47,48], and ingrowing nerves [49,50] as well as already formed primary or embryonic myofibers [51,52,53]. Many reports in the past indicated that developing skeletal muscle may release short-range signals that promote myogenesis in adjacent mesoderm cells [4,26,28,54,55,56]. In agreement with these data, the present study demonstrates *in vitro* that the foetal population originating from TNAP+ cells, unlike their postnatal counterpart, does not spontaneously undergo skeletal muscle differentiation, but it does so in the presence of surrounding skeletal muscle cells. Otherwise, the isolated TNAP+ cell-derived population mostly adopts a smooth muscle fate, which represents the default pathway for vascular progenitors.

5. Conclusions

TNAP+ cells found in prenatal skeletal muscle contribute to the formation of skeletal or smooth muscle cells, or pericytes, during muscle development. TNAP+ progenitors do not seem multipotent but rather heterogeneous unipotent progenitors. At variance with the post-natal derivatives, the foetal derivatives of TNAP+ cells require skeletal muscle-specific stimuli to achieve myogenic differentiation. Further investigation will allow to identify the signals tuning myogenesis in TNAP+ cells. Getting further knowledge on the clonal differentiation of these cells may help to get insights on the how their fate choices are physiologically modulated spatially and temporally, and how they can possibly be tuned for muscle regeneration purposes.

Funding

This project received funding from the European Union's Horizon 2020 research and innovation programme under the Marie Skłodowska-Curie grant agreement No. 860034.

CRedit authorship contribution statement

I. Fancello: Conceptualization, Data curation, Formal analysis, Investigation, Methodology, Writing original draft, review & editing. **S. Willett:** Investigation, Methodology. **C. Castiglioni:** Investigation, Methodology. **S. Amer:** Investigation, Methodology. **S. Santoleri:** Investigation, Methodology. **L. Bragg:** Project administration, Resources. **F. Galli:** Conceptualization, Data curation, Formal analysis, Supervision, Writing original draft, review & editing. **G. Cossu:** Conceptualization, Data curation, Formal analysis, Funding acquisition, Supervision, Roles/Writing - original draft, Writing - review & editing.

Declaration of competing interest

Authors declare they have no competing interests.

Appendix A. Supplementary data

Supplementary data to this article can be found online at <https://doi.org/10.1016/j.vph.2025.107489>.

Data availability

Data will be made available on request.

References

- [1] L. Díaz-Flores, R. Gutiérrez, J.F. Madrid, et al., Pericytes. Morphofunction, interactions and pathology in a quiescent and activated mesenchymal cell niche, *Histol. Histopathol.* 24 (7) (2009) 909–969, <https://doi.org/10.14670/HH-24.909>.
- [2] P.H. Dias Moura Prazeres, I. Fernandes Gilson Sena, Borges I. da Terra, et al., Pericytes are heterogeneous in their origin within the same tissue, *Dev. Biol.* 427 (1) (2017) 6–11, <https://doi.org/10.1016/j.ydbio.2017.05.001>.

- [3] O. Cappellari, G. Cossu, Pericytes in development and pathology of skeletal muscle, *Circ. Res.* 113 (3) (2013) 341–347, <https://doi.org/10.1161/CIRCRESAHA.113.300203>.
- [4] M.G. Minasi, M. Riminucci, Angelis L. De, et al., The meso-angioblast : a multipotent, self-renewing cell that originates from the dorsal aorta and differentiates into most mesodermal tissues, *Development* 129 (2002) 2773–2783, <https://doi.org/10.1242/dev.129.11.2773>.
- [5] G. Cossu, R. Tonlorenzi, S. Brunelli, et al., Mesoangioblasts at 20 : From the embryonic aorta to the patient bed, *Front. Genet.* 13 (2023) 1056114, <https://doi.org/10.3389/fgene.2022.1056114>.
- [6] A. Dellavalle, M. Sampaolesi, R. Tonlorenzi, et al., Pericytes of human skeletal muscle are myogenic precursors distinct from satellite cells, *Nat. Cell Biol.* 9 (3) (2007) 255–267, <https://doi.org/10.1038/ncb1542>.
- [7] A. Dellavalle, G. Maroli, D. Covarello, et al., Pericytes resident in postnatal skeletal muscle differentiate into muscle fibres and generate satellite cells, *Nat. Commun.* 2 (1) (2011) 499, <https://doi.org/10.1038/ncomms1508>.
- [8] A. Birbrair, T. Zhang, Z.M. Wang, et al., Role of pericytes in skeletal muscle regeneration and fat accumulation, *Stem Cells Dev.* 22 (16) (2013) 2298–2314, <https://doi.org/10.1089/scd.2012.0647>.
- [9] T. Tatsukawa, K. Kano, K.I. Nakajima, et al., NG2-positive pericytes regulate homeostatic maintenance of slow-type skeletal muscle with rapid myonuclear turnover, *Stem Cell Res Ther* 14 (1) (2023) 205, <https://doi.org/10.1186/s13287-023-03433-1>.
- [10] Y. Yoshida, M. Kabara, K. Kano, et al., Capillary-resident EphA7 + pericytes are multipotent cells with anti-ischemic effects through capillary formation, *Stem Cells Transl. Med.* 9 (2020) 120–130, <https://doi.org/10.1002/sctm.19-0148>.
- [11] K. Kano, K. Horiuchi, Y. Yoshida, et al., EphA7+ perivascular cells as myogenic and angiogenic precursors improving skeletal muscle regeneration in a muscular dystrophic mouse model, *Stem Cell Res.* 47 (January) (2020) 101914, <https://doi.org/10.1016/j.scr.2020.101914>.
- [12] U. Ozerdem, K.A. Grako, K. Dahlin-Huppe, E. Monosov, W.B. Stallcup, NG2 proteoglycan is expressed exclusively by mural cells during vascular morphogenesis, *Dev. Dyn.* 222 (2) (2001) 218–227, <https://doi.org/10.1002/dvdy.1200>.
- [13] P. Lindahl, B.R. Johansson, P. Leveen, C. Betsholtz, Pericyte loss and microaneurysm formation in PDGF-B-deficient mice, *Science* 277 (5323) (1997) 242–245, <https://doi.org/10.1126/science.277.5323.242>.
- [14] G.R. Macgregor, B.P. Zambrowicz, P. Soriano, Tissue non-specific alkaline phosphatase is expressed in both embryonic and extraembryonic lineages during mouse embryogenesis but is not required for migration of primordial germ cells, *Development* 121 (1995) 1487–1496, <https://doi.org/10.1242/dev.121.5.1487>.
- [15] K. Hoshi, N. Amizuku, K. Oda, Y. Ikehara, H. Ozawa, Immunolocalization of tissue non-specific alkaline phosphatase in mice, *Histochem. Cell Biol.* 107 (3) (1997) 183–191, <https://doi.org/10.1007/s004180050103>.
- [16] J. Livet, T.A. Weissman, H. Kang, et al., Transgenic strategies for combinatorial expression of fluorescent proteins in the nervous system, *Nature* 450 (7166) (2007) 56–62, <https://doi.org/10.1038/nature06293>.
- [17] H.J. Snippert, Flier L.G. Van Der, T. Sato, et al., Intestinal crypt homeostasis results from neutral competition between symmetrically dividing Lgr5 stem cells, *Cell* 143 (1) (2010) 134–144, <https://doi.org/10.1016/j.cell.2010.09.016>.
- [18] L. Dumas, S. Clavreul, F. Michon, K. Loulier, Multicolor strategies for investigating clonal expansion and tissue plasticity, *Cell. Mol. Life Sci.* 79 (3) (2022) 141, <https://doi.org/10.1007/s00018-021-04077-1>.
- [19] D. Sakry, J. Trotter, The role of the NG2 proteoglycan in OPC and CNS network function, *Brain Res.* 1638 (2016) 161–166, <https://doi.org/10.1016/j.brainres.2015.06.003>.
- [20] J.I. Fukushi, M. Inatani, Y. Yamaguchi, W.B. Stallcup, Expression of NG2 proteoglycan during endochondral and intramembranous ossification, *Dev. Dyn.* 228 (1) (2003) 143–148, <https://doi.org/10.1002/dvdy.10359>.
- [21] W.B. Stallcup, The NG2 proteoglycan in pericyte biology, *Adv. Exp. Med. Biol.* 1109 (2018) 5–19, https://doi.org/10.1007/978-3-030-02601-1_2.
- [22] K.J. Mitchell, A. Pannérec, B. Cadot, et al., Identification and characterization of a non-satellite cell muscle resident progenitor during postnatal development, *Nat. Cell Biol.* 12 (3) (2010) 256–266, <https://doi.org/10.1038/ncb2025>.
- [23] N. Liu, G.A. Garry, S. Li, et al., A Twist2-dependent progenitor cell contributes to adult skeletal muscle, *Nat. Cell Biol.* 19 (3) (2017) 202–213, <https://doi.org/10.1038/ncb3477>.
- [24] C.G.K. Flynn, P.R. Van Ginkel, K.A. Hubert, et al., Hox11-expressing interstitial cells contribute to adult skeletal muscle at homeostasis, *Development* 150 (4) (2023), <https://doi.org/10.1242/dev.201026>.
- [25] M. Esner, S.M. Meilhac, F. Relaix, J.F. Nicolas, G. Cossu, M.E. Buckingham, Smooth muscle of the dorsal aorta shares a common clonal origin with skeletal muscle of the myotome, *Development* 133 (4) (2006) 737–749, <https://doi.org/10.1242/dev.02226>.
- [26] G. Ugarte, O. Cappellari, L. Perani, A. Pistocchi, G. Cossu, Noggin recruits mesoderm progenitors from the dorsal aorta to a skeletal myogenic fate, *Dev. Biol.* 365 (1) (2012) 91–100, <https://doi.org/10.1016/j.ydbio.2012.02.015>.
- [27] M. Lagha, S. Brunelli, G. Messina, A. Cumano, T. Kume, F. Relaix, M. E. Buckingham, Pax3:Foxc2 reciprocal repression in the somite modulates muscular versus vascular cell fate choice in multipotent progenitors, *Dev. Cell* 17 (6) (2009) 892–899, <https://doi.org/10.1016/j.devcel.2009.10.021>.
- [28] F. Relaix, D. Montarras, S. Zaffran, et al., Pax3 and Pax7 have distinct and overlapping functions in adult muscle progenitor cells, *J. Cell Biol.* 172 (1) (2006) 91–102, <https://doi.org/10.1083/jcb.200508044>.
- [29] G. Messina, G. Cossu, The origin of embryonic and fetal myoblasts: a role of Pax3 and Pax7, *Genes Dev.* 23 (8) (2009) 902–905, <https://doi.org/10.1101/gad.1797009>.
- [30] A. Armulik, G. Genové, C. Betsholtz, Pericytes: developmental, physiological, and pathological perspectives, problems, and promises, *Dev. Cell* 21 (2) (2011) 193–215, <https://doi.org/10.1016/j.devcel.2011.07.001>.
- [31] S.F. Gilbert, Epigenetic landscaping: Waddington's use of cell fate bifurcation diagrams, *Biol. Philos.* 6 (1991) 135–154, <https://doi.org/10.1007/BF02426835>.
- [32] L. Gambardella, Y. Barrandon, The multifaceted adult epidermal stem cell, *Curr. Opin. Cell Biol.* 15 (6) (2003) 771–777, <https://doi.org/10.1016/j.ceb.2003.10.011>.
- [33] S.C. Lodestijn, T. van den Bosch, L.E. Nijman, et al., Continuous clonal labeling reveals uniform progenitor potential in the adult exocrine pancreas, *Cell Stem Cell* 28 (11) (2021) 2009–2019.e4, <https://doi.org/10.1016/j.stem.2021.07.004>.
- [34] E. Kostallari, Y. Baba-Amer, S. Alonso-Martin, et al., Pericytes in the myovascular niche promote post-natal myofiber growth and satellite cell quiescence, *Development* 142 (7) (2015) 1242–1253, <https://doi.org/10.1242/dev.115386>.
- [35] B. Mierzejewski, I. Grabowska, D. Jackowski, et al., Mouse CD146+ muscle interstitial progenitor cells differ from satellite cells and present myogenic potential, *Stem Cell Res Ther* 11 (2020) 341, <https://doi.org/10.1186/s13287-020-01827-z>.
- [36] L. Muhl, G. Genové, S. Leptidis, et al., Single-cell analysis uncovers fibroblast heterogeneity and criteria for fibroblast and mural cell identification and discrimination, *Nat. Commun.* 11 (1) (2020) 1–18, <https://doi.org/10.1038/s41467-020-17740-1>.
- [37] M. Ikeya, S. Takada, Wnt signaling from the dorsal neural tube is required for the formation of the medial dermomyotome, *Development* 125 (24) (1998) 4969–4976, <https://doi.org/10.1242/dev.125.24.4969>.
- [38] A.E. Münsterberg, J. Kitajewski, D.A. Bumcrot, A.P. McMahon, A.B. Lassar, Combinatorial signaling by sonic hedgehog and Wnt family members induces myogenic bHLH gene expression in the somite, *Genes Dev.* 9 (23) (1995) 2911–2922, <https://doi.org/10.1101/gad.9.23.2911>.
- [39] H.M. Stern, A.M.C. Brown, S.D. Hauschka, Myogenesis in paraxial mesoderm: preferential induction by dorsal neural tube and by cells expressing Wnt-1, *Development* 121 (11) (1995) 3675–3686, <https://doi.org/10.1242/dev.121.11.3675>.
- [40] G. Cossu, R. Kelly, S. Tajbakhsh, S. Di Donna, E. Vivarelli, M. Buckingham, Activation of different myogenic pathways: myf-5 is induced by the neural tube and MyoD by the dorsal ectoderm in mouse paraxial mesoderm, *Development* 122 (2) (1996) 429–437, <https://doi.org/10.1242/dev.122.2.429>.
- [41] C. Marcelle, M.R. Stark, M. Bronner-Fraser, Coordinate actions of BMPs, Wnts, Shh and noggin mediate patterning of the dorsal somite, *Development* 124 (20) (1997) 3955–3963, <https://doi.org/10.1242/dev.124.20.3955>.
- [42] A.C. Rios, O. Serralbo, D. Salgado, C. Marcelle, Neural crest regulates myogenesis through the transient activation of NOTCH, *Nature* 473 (7348) (2011) 532–535, <https://doi.org/10.1038/nature09970>.
- [43] S.S. Rayagiri, D. Ranaldi, A. Raven, et al., Basal lamina remodeling at the skeletal muscle stem cell niche mediates stem cell self-renewal, *Nat. Commun.* 9 (1) (2018) 1–12, <https://doi.org/10.1038/s41467-018-03425-3>.
- [44] A.-G. Borycki, The myotomal basement membrane: insight into laminin-111 function and its control by sonic hedgehog signaling, *Cell Adhes. Migr.* 7 (1) (2013) 72–81, <https://doi.org/10.4161/cam.23411>.
- [45] M.T. Tierney, A. Gromova, F. Boscolo Sesillo, et al., Autonomous extracellular matrix remodeling controls a progressive adaptation in muscle stem cell regenerative capacity during development, *Cell Rep.* 14 (8) (2016) 1940–1952, <https://doi.org/10.1016/j.celrep.2016.01.072>.
- [46] A. Armulik, A. Abramsson, C. Betsholtz, Endothelial/pericyte interactions, *Circ. Res.* 97 (6) (2005) 512–523, <https://doi.org/10.1161/01.RES.0000182903.16652.d7>.
- [47] O. Cappellari, S. Benedetti, A. Innocenzi, et al., Dll4 and PDGF-BB convert committed skeletal myoblasts to pericytes without erasing their myogenic memory, *Dev. Cell* 24 (6) (2013) 586–599, <https://doi.org/10.1016/j.devcel.2013.01.022>.
- [48] M.F.M. Gerli, L.A. Moyle, S. Benedetti, et al., Combined Notch and PDGF signaling enhances migration and expression of stem cell markers while inducing perivascular cell features in muscle satellite cells, *Stem Cell Rep.* 12 (3) (2019) 461–473, <https://doi.org/10.1016/j.stemcr.2019.01.007>.
- [49] P.M. Rodríguez Cruz, J. Cossins, D. Beeson, A. Vincent, The neuromuscular junction in health and disease: molecular mechanisms governing synaptic formation and homeostasis, *Front. Mol. Neurosci.* 13 (2020) 610964, <https://doi.org/10.3389/fnmol.2020.610964>.
- [50] J. Delezie, M. Weirauch, G. Maier, et al., BDNF is a mediator of glycolytic fiber-type specification in mouse skeletal muscle, *Proc. Natl. Acad. Sci. USA* 116 (32) (2019) 16111–16120, <https://doi.org/10.1073/pnas.1900544116>.
- [51] S. Biresi, M. Molinaro, G. Cossu, Cellular heterogeneity during vertebrate skeletal muscle development, *Dev. Biol.* 308 (2007) 281–293, <https://doi.org/10.1016/j.ydbio.2007.06.006>.
- [52] M. Buckingham, S.D. Vincent, Distinct and dynamic myogenic populations in the vertebrate embryo, *Curr. Opin. Genet. Dev.* 19 (2009) 444–453, <https://doi.org/10.1016/j.gde.2009.08.001>.
- [53] G. Comai, S. Tajbakhsh, Molecular and cellular regulation of skeletal myogenesis, *Curr. Top. Dev. Biol.* 110 (2014), <https://doi.org/10.1016/B978-0-12-405943-6.00001-4>.

- [54] R.S. Krauss, G.A. Joseph, A.J. Goel, Keep your friends close: cell–cell contact and skeletal myogenesis, *Cold Spring Harb. Perspect. Biol.* 9 (2017) a029298, <https://doi.org/10.1101/cshperspect.a029298>.
- [55] S.J. Bray, Notch signalling: a simple pathway becomes complex, *Nat. Rev. Mol. Cell Biol.* 7 (9) (2006) 678–689, <https://doi.org/10.1038/nrm2009>.
- [56] D. Costamagna, H. Mommaerts, M. Sampaolesi, P. Tylzanowski, Noggin inactivation affects the number and differentiation potential of muscle progenitor cells in vivo, *Sci. Rep.* 6 (August) (2016) 31949, <https://doi.org/10.1038/srep31949>.